

MUTUAL COUPLING BETWEEN A PAIR OF IDENTICAL BEAM STEERING DIELECTRIC RESONATOR ANTENNAS

H. Fayad and P. Record

Department of Electrical, Electronics and Computer Engineering
Heriot-Watt University
Edinburgh, EH14 4AS, UK

Abstract—A comparative study using numerical models on the mutual coupling (MC) between two different heterogeneous beam steering dielectric resonator antennas (DRAs) and an omni-directional dielectric resonator antenna (DRA) is presented in this paper. The mutual coupling was investigated by varying the separation between the antennas and manipulating the far field radiation pattern of each antenna. Several arrangements with element separation ranging from 0.1 to 0.5 free space wave length were investigated at the design frequency of 10 GHz. Different configurations contributed to different isolation levels. It was found that a significant isolation (< -15 dB) between an array of heterogeneous DRAs can be obtained even with antennas placed in close proximity (0.1 free space wavelength separation). It was also shown that the resonant frequency and return loss are most affected at settings where the direction of the main lobe of antenna A overlaps with the direction of the main lobe of antenna B. The expected inverse proportionality between ‘ d ’ (the separation between two antennas) and the level of MC was also demonstrated.

1. INTRODUCTION

Mutual coupling (MC) or isolation is a term that describes the electromagnetic wave EMW interaction between antennas placed in close proximity [1]. This interaction causes some consequences on the antennas’ characteristics including distortion of the radiation pattern, input impedance, gain and efficiency. Hence, it is an important figure of merit in a number of applications; these include antenna arrays

Corresponding author: H. Fayad (hazem.fayad@jpkaberdeen.com).

and MIMO (Multiple Input Multiple Output) systems which consist of a number of antennas to offer an increase in capacity without the need for an additional bandwidth compared to conventional system [2]. The effect of MC on channel capacity of a MIMO system is still an active area for research. It has been shown in [2–4] that the better the isolation between antenna arrays, the higher is MIMO system capacity.

Enhancing the level of isolation between two identical antennas placed in close proximity has attracted considerable interest over the last decade and several methods have been reported. Authors in [4] improved the isolation between two adjacent planar inverted F antenna (PIFAs) by introducing a small ground plane to each antenna before mounting it directly on the printed circuit board (PCB) (with an air gap between the PCB and ground plane). This design reduced the electromagnetic coupling between the antenna and the PCB; giving > 20 dB isolation between the two radiating elements that were placed $0.17\lambda_o$ apart. Rikuta and Arain suppressed the MC in [5] by using antennas with high Front-to-Back ratio. The front to back ratio was enhanced by adding reflectors to two dipoles to enhance their directivity. Level of MC was suppressed by changing length, width, shape of the reflector. It was shown that the higher the Front-to-Back ratio, the lower is the MC between the type of antennas studied in [6]. This demonstrated that the radiation pattern of the antenna plays a significant role in MC level.

MC between dielectric resonator antenna (DRAs) have been studied in the past by some researchers [7–9]. The MC between two hemispherical DRAs (H-DRAs) has been analyzed theoretically in [7] by Luk et al. It has been shown in this context that the mutual coupling (~ -12.5 dB for ~ 0.4 free space wavelength) is significant and should be taken into account when designing an array of H-DRAs. Chair et.al reported in [8] a rigorous study on the MC between two cylindrical DRAs for different radius to height ratio (r/H), (antennas were excited in the broad side mode by a coaxial cable). Results showed that isolation was decreased as the ratio of (r/H) was reduced. Two dB improvement in MC was reported when radius was decreased from 4.2 mm to 2.98 mm (distance between antennas was 0.4 free space wavelength). Few of the publications on the MC of DRAs analyzed the different shapes and feeding mechanism; however to the author's knowledge no published work has been reported on the level of MC between identical beam-steering DRAs of the type described in this paper. This work extends our previous work on beam steering DRAs [10–13].

The main objective of this paper is to report the isolation level between a pair of identical beam steering DRAs compared to an omni-

directional DRA. MC of three different prototypes was investigated; these include: i) MC between a pair of homogeneous cylindrical DRA with omni-directional radiation pattern (Section 2.1), ii) MC between Heterogeneous beam steering DRA as described in Section 2.2, iii) MC between a pair of Multi-feed DRA with reconfigurable radiation pattern. as described in Section 2.3.

2. ANALYSIS OF MC OF DIFFERENT ANTENNA PROTOTYPES

2.1. Homogeneous Cylindrical DRA (C-DRA)

Two identical cylindrical DRAs were modeled in Ansoft HFSS version 9 and their MC was determined. The antennas had a resonant frequency of 10 GHz, and the relative permittivity of the material chosen was 6.5. Radius (r) of the homogeneous C-DRA was 8.3 mm and height (h) was 6.8 mm. Antennas were fed by a gold electrode of radius 0.65 mm and height 5.88 mm protruded into the base of the dielectric cylinder to excite the dielectric media. Central excitation was chosen to excite TM mode.

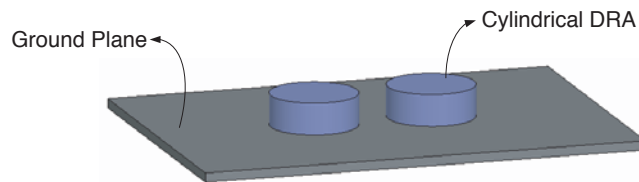


Figure 1. 3D view of the antennas under study (two identical Homogeneous C-DRA mounted on a ground plane).

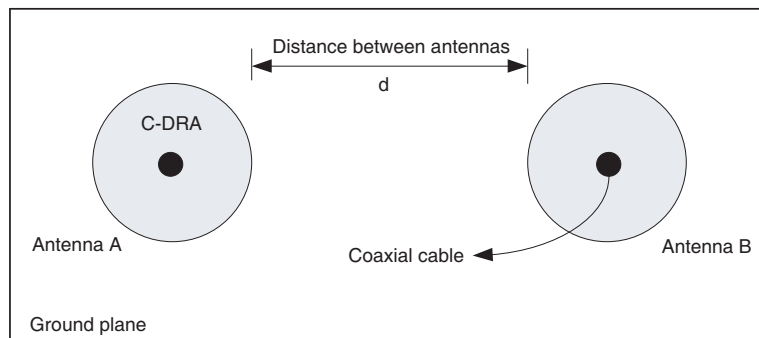


Figure 2. Top view of the antennas under study.

The overall geometry of this structure is shown in Fig. 1. Fig. 2 shows a top view of the antenna array under study. Because the various antenna structures investigated in this paper had different dimensions but share the same resonant frequency (10 GHz), it was thought that the separation ‘ d ’ between antennas, defined as the distance between the outer-surfaces adjacent to each other, is the best parameter for comparison, Fig. 2. Fig. 3 is a plot of the antenna return loss for various values of ‘ d ’. It can be seen that the antenna return loss varies significantly as the separation between the two antennas (A & B) decreases. Fig. 4 describes the level of MC between A & B; it shows how the MC varies with frequency and with antenna separation. As was expected, the level of MC increases as the distance between A & B decreases.

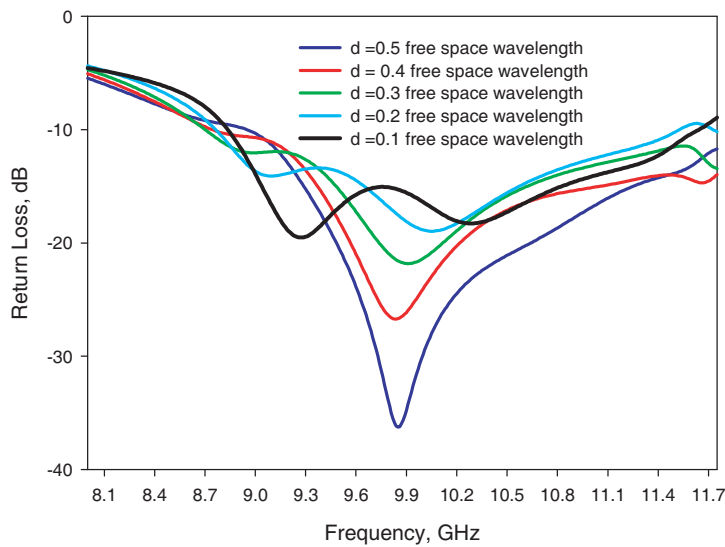


Figure 3. Return loss of the antenna for various values of ‘ d ’.

2.2. Heterogeneous Beam Steering Dielectric Resonator Antenna

We have described in our previous work [11] a heterogeneous beam steering dielectric resonator antenna operating at ~ 1.2 GHz. The antenna consisted of a movable heterogeneous dielectric shell surrounding a core of another dielectric. It was found that the direction of radiation could be controlled by physically moving the heterogeneous dielectric shell in the azimuth plane. In a cylindrical structure this

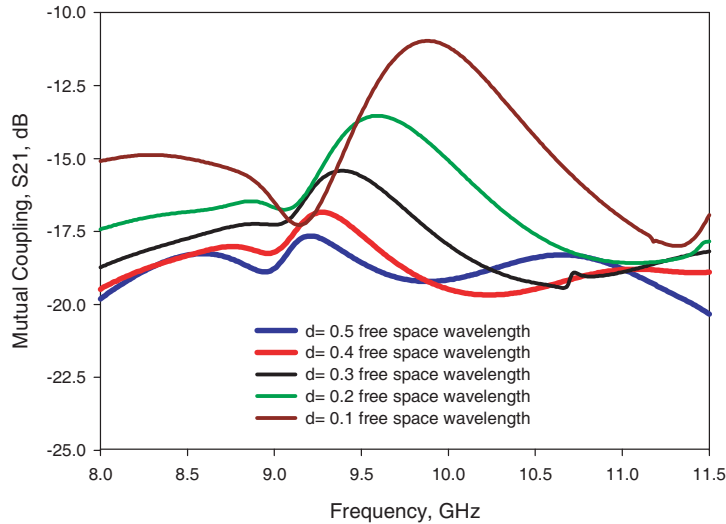


Figure 4. MC versus the separation ‘ d ’ between the two antennas various frequencies.

gave 360 degree rotation in the azimuth plane and for a hemispherical structure [12] 90 degrees in the elevation plane. It has been shown in our previous published work [11] that good agreement is obtained between simulation from HFSS modeling and measurement which verified the effectiveness of modeling heterogeneous DRAs using Ansoft HFSS.

Although the results presented in [10,11] were conducted at different frequency band however these results in no way limit the frequency of operation since low losses dielectrics are available up to 110 GHz. Cylindrical structure was chosen to compare the results of the heterogeneous Beam-steering DRA (resonating at 10 GHz) with the homogeneous C-DRA studied in Subsection 2.1. Figs. 5(a) and (b) is a 3D view and side view respectively of the heterogeneous C-DRA. Section 2.1 had a relative permittivity of 20, inner radius ‘ C ’ of 2.1, outer radius ‘ B ’ of 5.5 mm and height ‘ h ’ of 2.4 mm; surrounded by a movable annulus of heterogeneous dielectric sections. Sections 2, 3 and 4 had a relative permittivity of 110 and the permittivity of Section 1 was 20. The outer ring had an inner radius of 5.5 mm and outer radius 7.46 mm and height 2.4 mm. The antenna was excited at the centre by an SMA connector of radius 0.653 mm and height 4.5 mm.

Figures 6 and 7 are 3D view and top view respectively of the antenna array under study. Because the heterogeneous antenna has

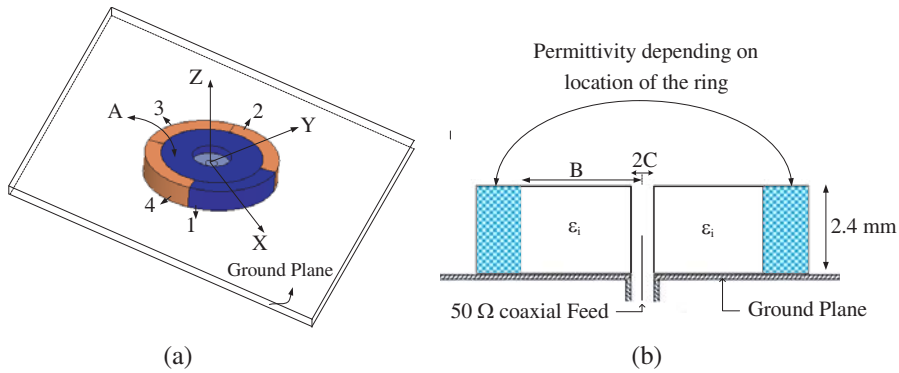


Figure 5. (a) 3D view of one heterogeneous C-DRA. (b) Side view of the heterogeneous C-DRA.

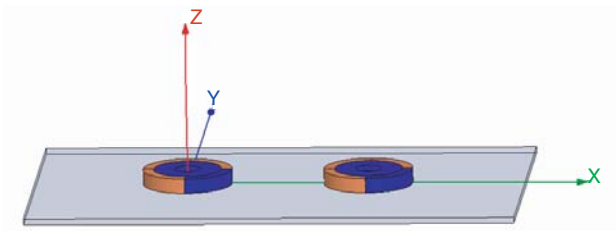


Figure 6. Geometry of the antennas under study (two identical heterogeneous C-DRA mounted on a ground plane; ring of both antennas is rotated -45 degrees compared to the reference position shown in Fig. 5(a).

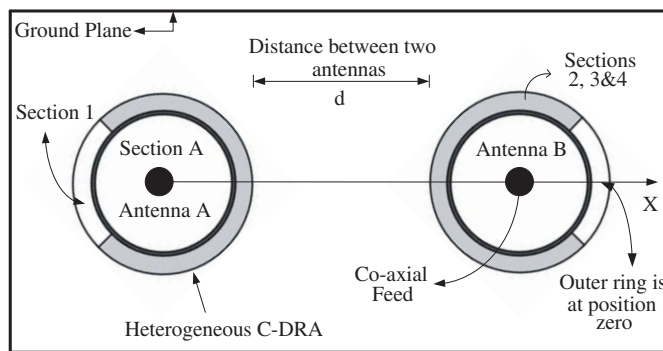
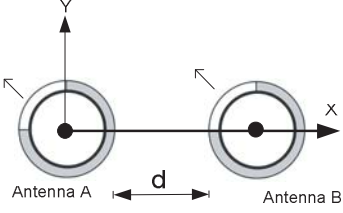
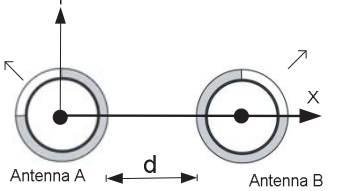
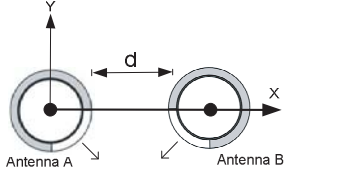


Figure 7. Top view of the antennas; outer ring of Antenna A is rotated 180 degrees and the outer ring of Antenna B is at zero degree, with respect to the reference position of the ring shown in Fig. 5(a).

Table 1. Different case studies investigated.

Case Number	Location of the outer ring; arrows shows the direction of the main lobe	Location of the outer ring with respect to the reference position shown in Fig. 5(a)
Case 1		(A, 135) and (B, 135)
Case 2		(A, 135) and (B, 45)
Case 3		(A, 315) and (B, 225)

beam-steering characteristics; a subset of ring positions was considered to fully describe the coupling behavior; this is illustrated in Table 1.

Isolation levels for case number 1, Table 1, was investigated by varying the separation ‘ d ’ between the two antennas. Fig. 8 shows the simulated results for the antenna return loss versus various separation between Antenna A and B, and the MC level is given in Fig. 9. Fig. 9 shows that the level of MC was decreased as the distance between both antennas increased. Comparing these MC, Fig. 9, to those shown in Fig. 4; it can be seen that the isolation between the Beam Steering heterogeneous DRA (for $d = 0.1\lambda_o$) was better (by ~ 8 dB) compared to that seen with the homogeneous DRA for the same separation distance.

For comparison, two more investigations have been studied. For the case (A, 135) and (B, 45) (case number 2, Table 2), the return

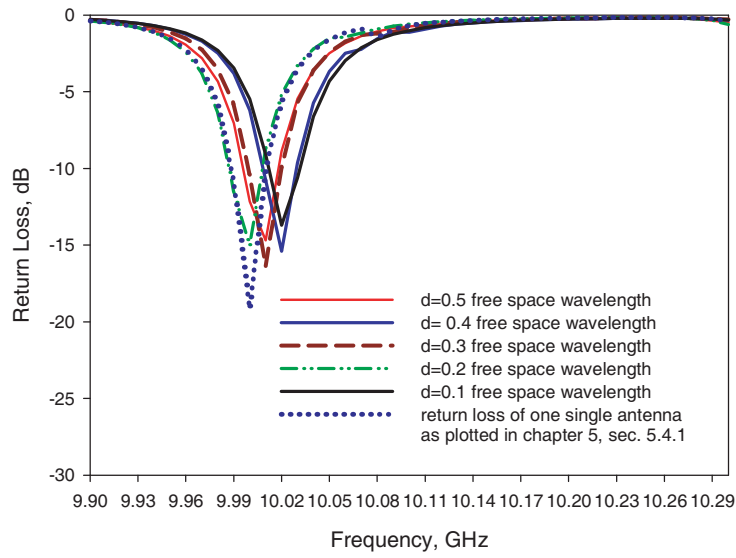


Figure 8. Return loss versus antenna separation for case study No. 1.

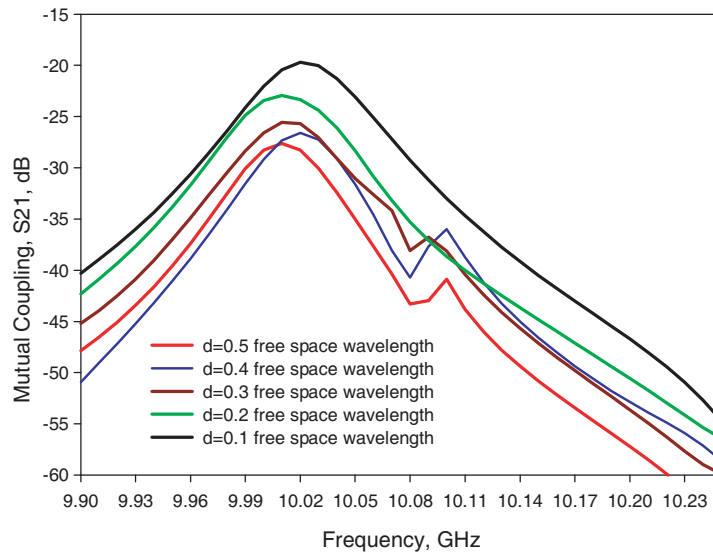


Figure 9. MC versus separation ' d ' for case study number 1 as described.

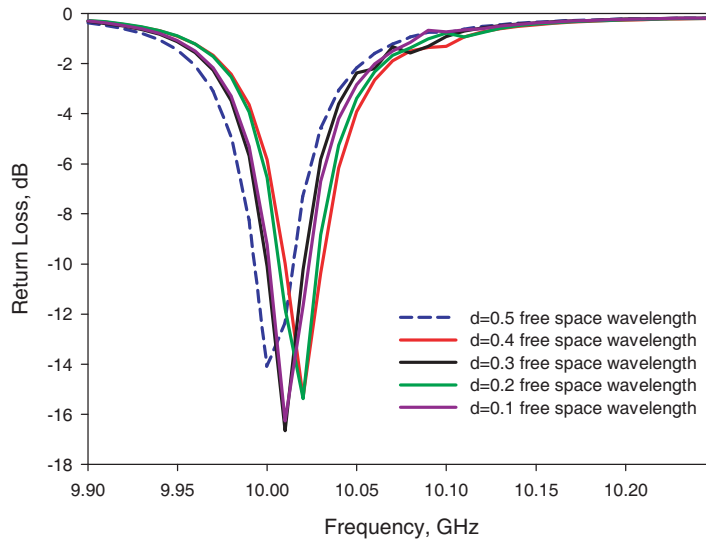


Figure 10. Return Loss for various antenna separation ' d ' for case study number 2.

loss and isolation level were plotted in Fig. 10 and Fig. 11 respectively. Comparing these isolation levels (Fig. 11) to those plotted in Fig. 9, it can be seen that the isolation level of case number 2 was better compared to that of case number 1. Results were predicted due to the fact that the near field interaction between both antennas in case 2 was less compared to that of case 1. However, both cases demonstrated that a pair of identical beam steering antennas provides a significant improvement of isolation of ~ 8 dB and 18 dB respectively for cases 1 & 2 respectively and for $d = 0.1\lambda_o$, compared to the homogeneous C-DRA described in Section 2.1 (for $d = 0.1\lambda_o$); this is illustrated in Fig. 12.

For the case (A, 315) and (B, 225) (case number 3, Table 2, the return loss and the isolation level were plotted in Fig. 13 and Fig. 14 respectively. The positions of the outer rings demonstrated that the radiation pattern of each antenna was directed towards the adjacent element, and hence the level of MC in this case was expected to be higher compared to previous configurations (case No. 2 & 3). Even though the isolation level of case No. 3 is lower than that of the homogeneous C-DRA for $d = 0.1$ free space wavelength; however, Fig. 13 shows that the return loss deteriorates significantly for values of ' d ' below 0.2 free space wavelength. The spectra of the homogeneous

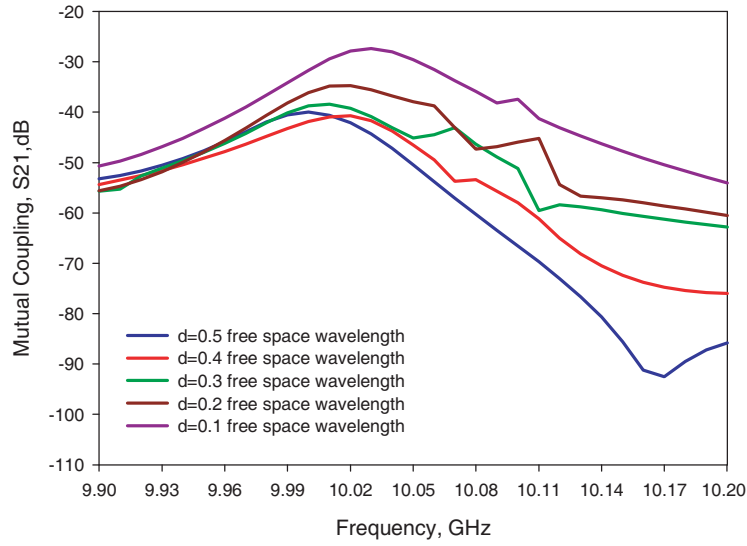


Figure 11. Level of MC between identical antennas for case study No. 2.

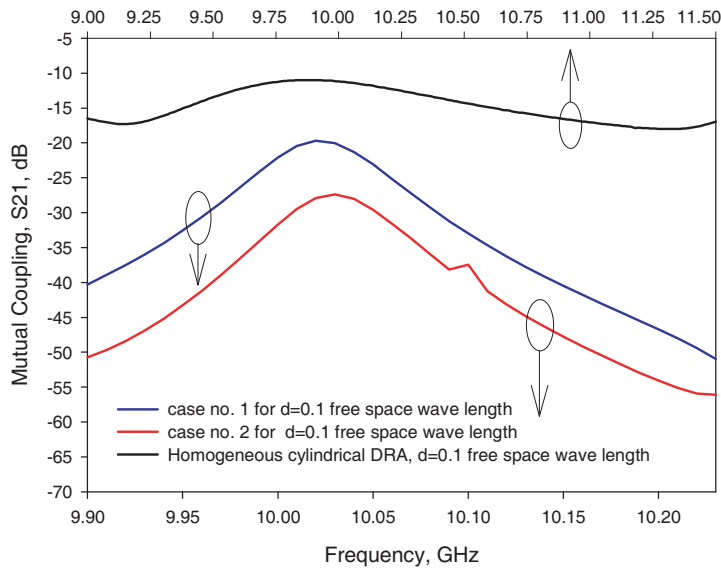


Figure 12. Comparison of the MC for various antenna structures, for $d = 0.1$ free space wavelength.

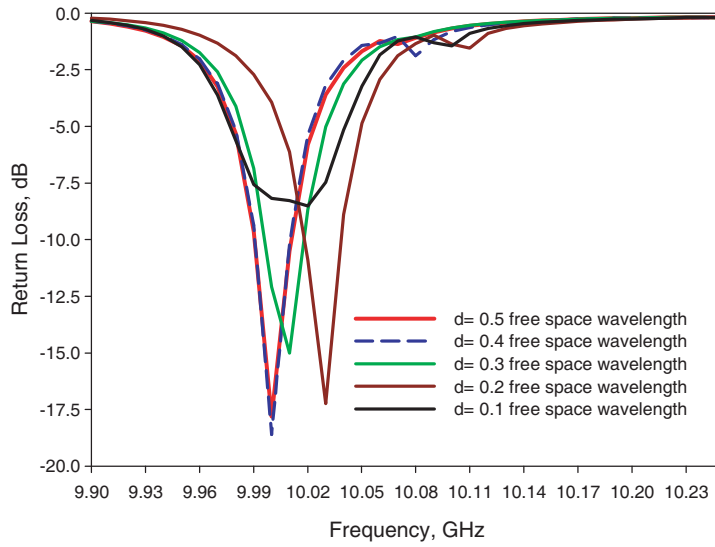


Figure 13. Return loss versus separation 'd' for case study number 3.

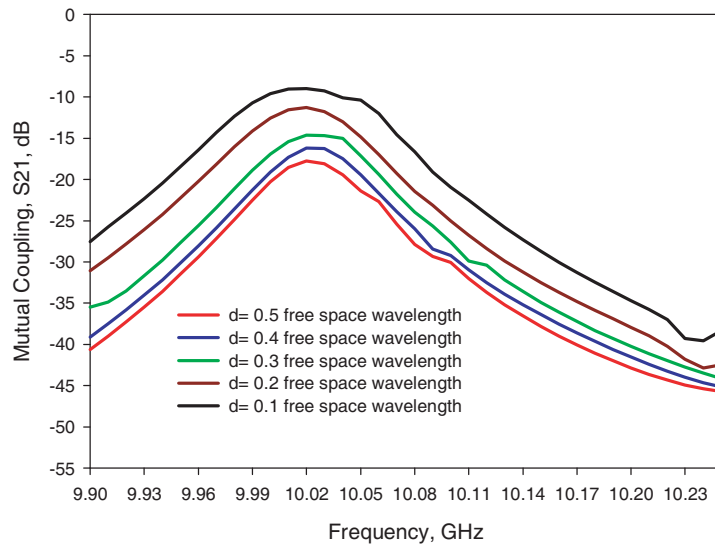


Figure 14. MC between antennas for case study number 3.

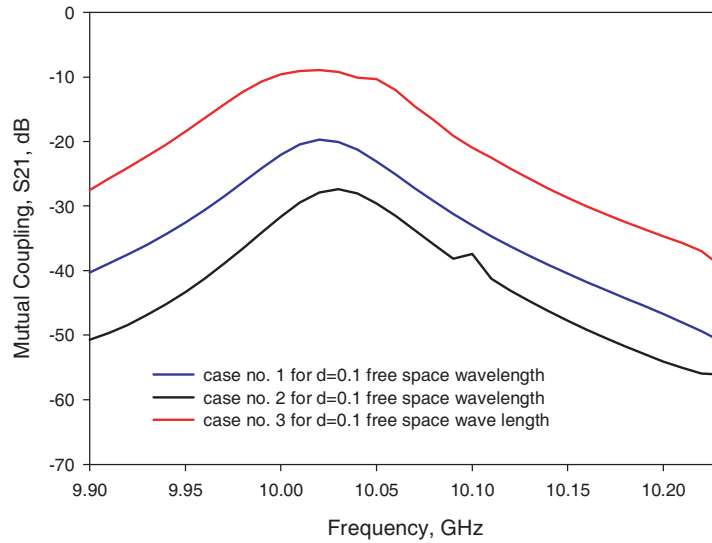


Figure 15. Isolation level of three different cases for $d = 0.1$ free space wavelength.

C-DRA was completely different for the same separation since more resonances emerged, see Fig. 3. It is believed that more modes were stimulated in the homogeneous C-DRA array due to the coupling between the adjacent elements.

From the results presented in this section, it can be seen that the position of the outer ring of one antenna relative to the position of the outer ring of the adjacent antenna has a positive/negative impact on the level of MC. Fig. 15 is a plot of the isolation level of the three different cases (1, 2 & 3) for $d = 0.1$ free space wave length. It is to be noted that even though more than three different scenarios can be considered, however, it is believed that these three cases give a good estimation about the isolation levels of these types of antennas.

2.3. Multi Feed Beam Steering Antenna

The beam steering antenna presented in this subsection comprised of a hollow cylindrical DRA fed by four orthogonally positioned probes. The antenna's characteristics were described in our previous published work in [13]. Fig. 16 shows a snap shot of the antenna prototype, and Fig. 17 shows the simulated versus measured results for this antenna when only one probe was activated while other probes were open circuited. The dielectric pellet had a relative permittivity of 6, inner

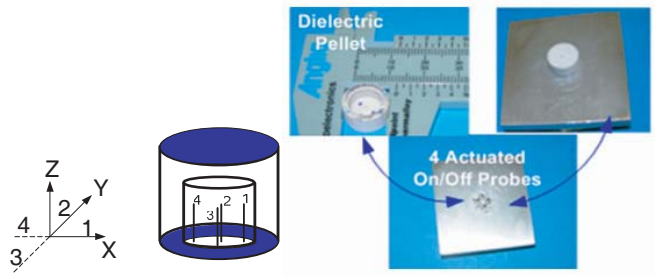


Figure 16. Beam steering Multi feed DRA.

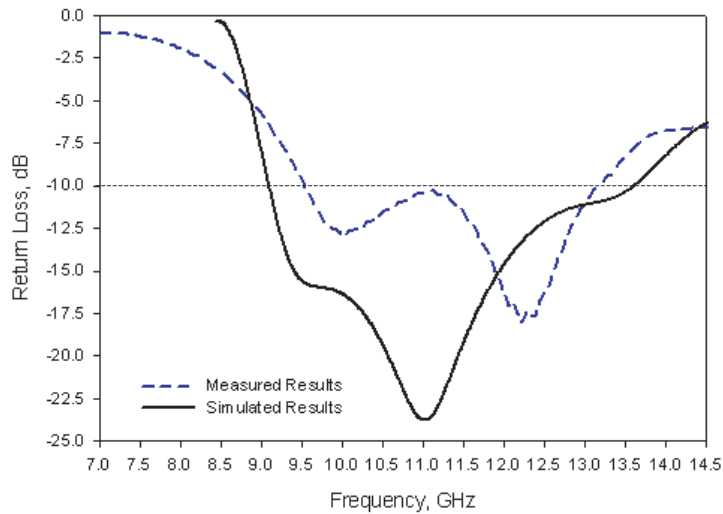


Figure 17. Simulation versus measured results for the return loss.

radius ‘ C ’ of 4.6 mm ($0.17\lambda_0$) and outer radius ‘ B ’ of 6.6 mm ($0.24\lambda_0$). The inner height ‘ h ’ was 3.9 mm ($0.14\lambda_0$) and the outer height ‘ H ’ was 6.8 mm ($0.25\lambda_0$). Four gold electrodes of radius 0.653 mm and height ‘ L ’ 3.88 mm extended into the hollow cylinder to achieve 50Ω matching impedance. The four probes were located on a radius of distance ‘ d ’, 1.6 mm, from the centre of the electrodes to the inner surface of the cylinder. Figs. 18 and 19 is an overall geometry and top view of the antenna array under study. Similarly to the last antenna study, a subset of probe excitation represents various levels of MC between these antennas; Table 2 illustrates the different scenarios investigated.

Results of return loss and isolation levels for case studies A-C

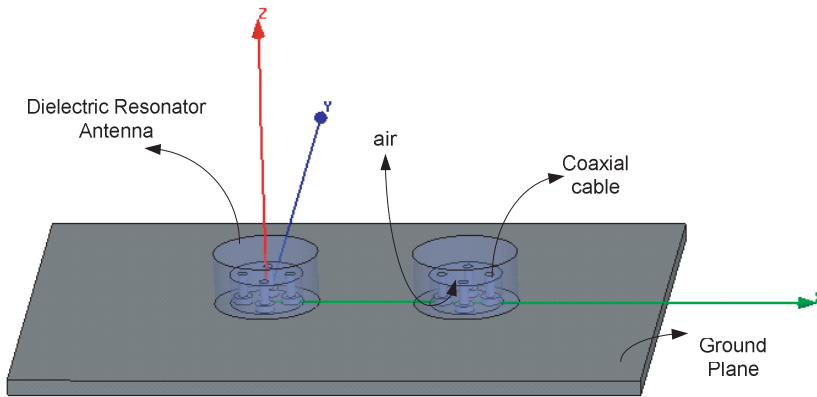


Figure 18. Geometry of the antenna array.

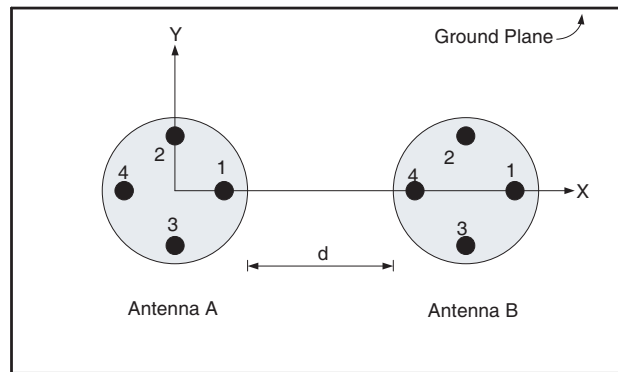


Figure 19. Side view of the antenna array and the number of probes allocated within the dielectric.

are plotted in Fig. 20–Fig. 25. It is seen that the resonant frequency and return loss of this antenna was hardly deteriorated for the various scenarios investigated. Fig. 26 compares the isolation level of the three cases (A, B and C) for $d = 0.1$ free space wave length with that of the homogeneous C-DRA for the same separation distance. It is seen that the multi-feed DRA in the worse case scenario (case B) only provides better isolation of ~ 2.5 dB compared to the homogeneous cylindrical DRA.

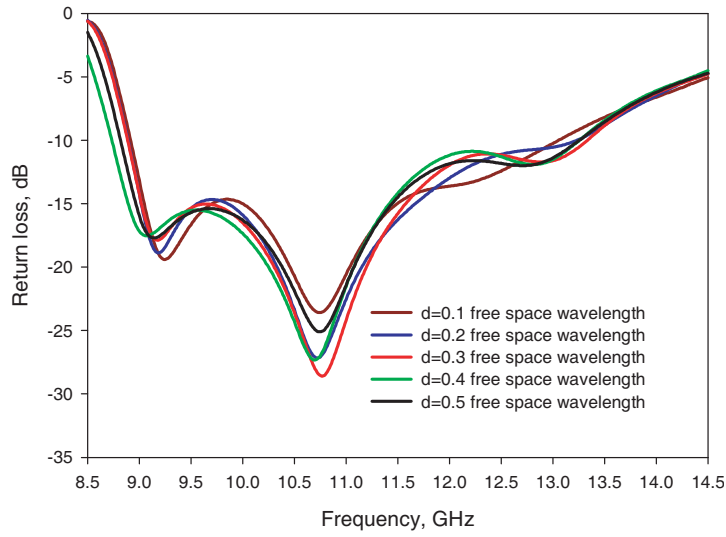


Figure 20. Case A: Return loss of the antenna array versus separation ‘ d ’ for the case study A.

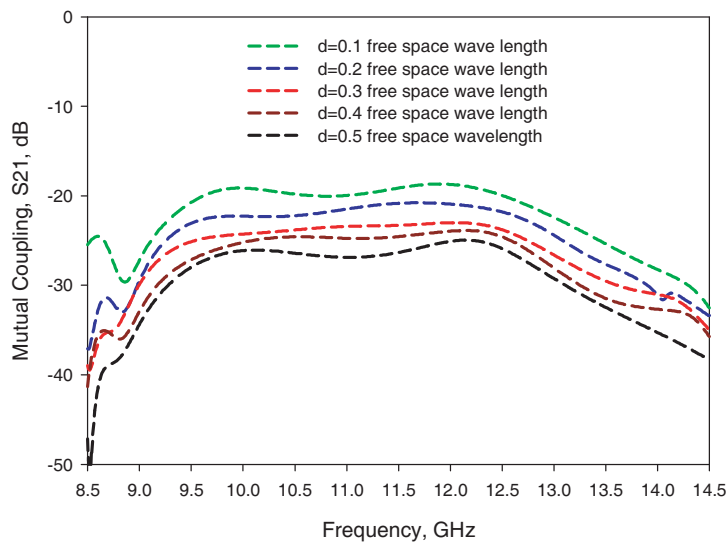


Figure 21. Case A: MC between the two antennas versus separation ‘ d ’ for the case study A.

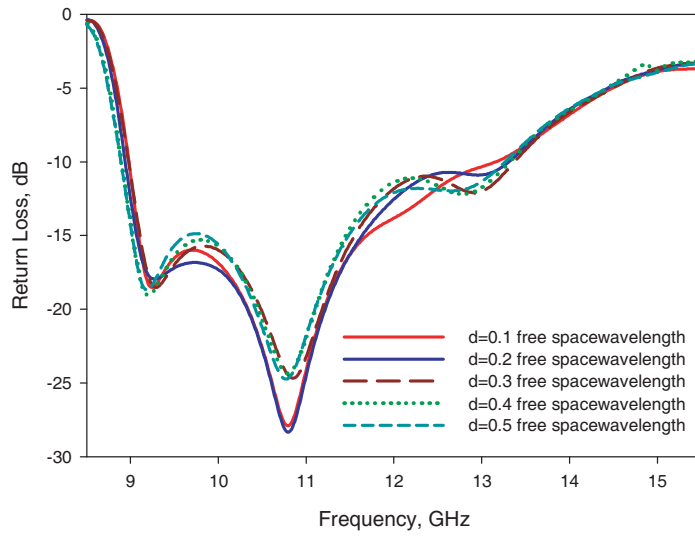


Figure 22. Case B: Return loss of the antenna array versus separation ' d ' for the case study B.

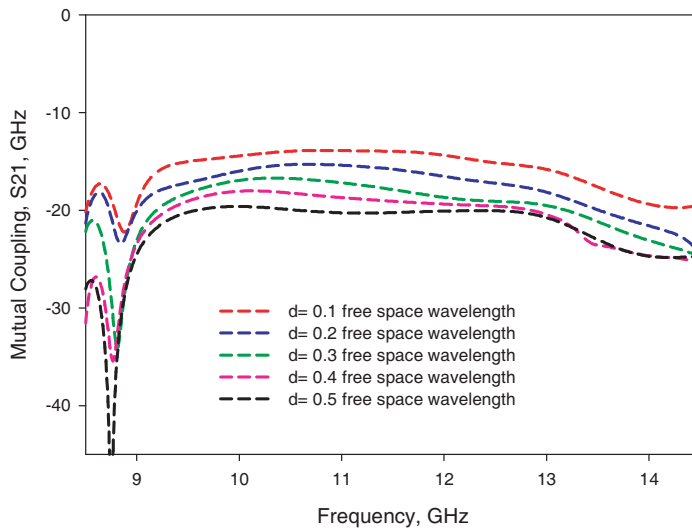


Figure 23. Case B: MC between the two antennas versus separation ' d ' for the case study B.

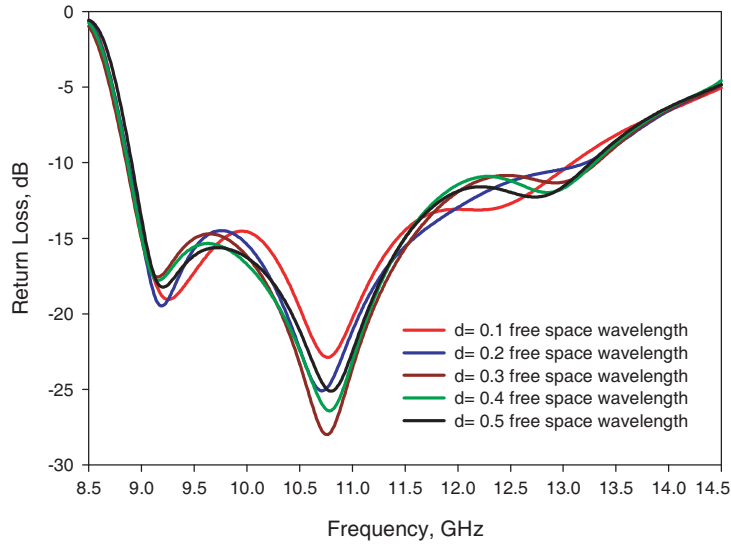


Figure 24. 1 Case C: Return loss of the antenna array versus separation.

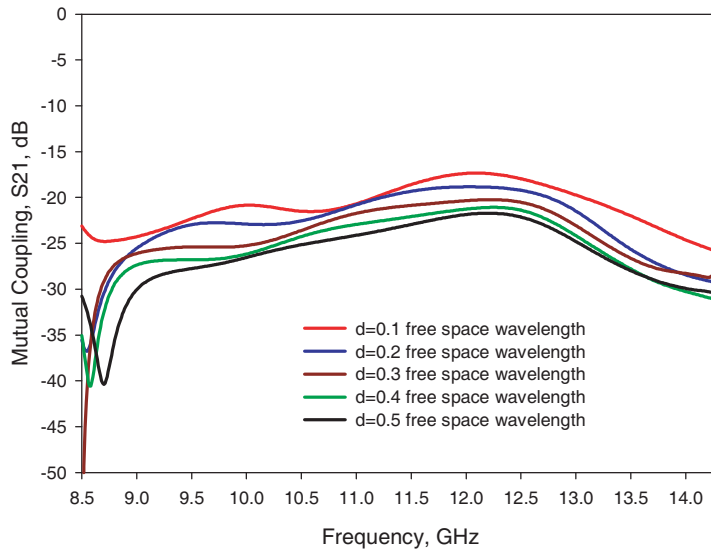


Figure 25. Case C: MC between the two antennas versus separation 'd' for the case study C.

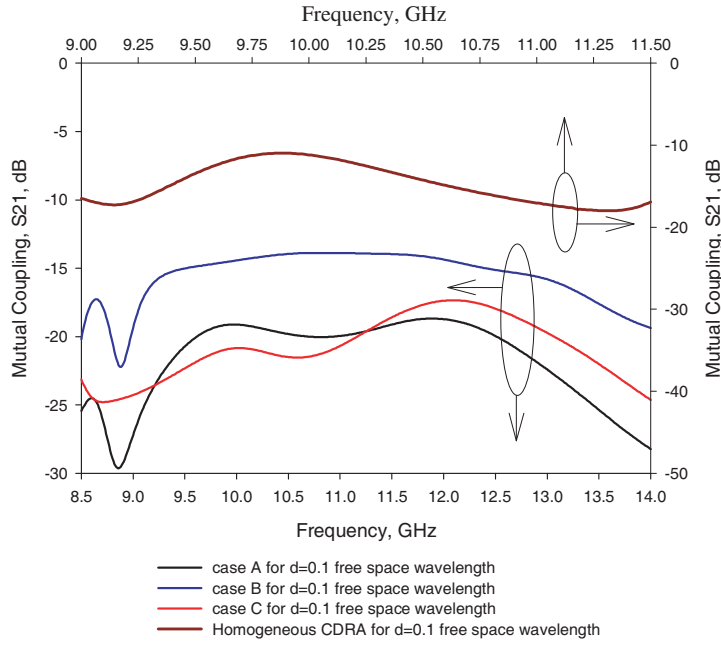


Figure 26. Comparison of the isolation level of the Multi-feed DRA with the homogeneous DRA for $d = 0.1$ free space wavelength.

Table 2. Different case studies investigated.

Case Number	Location of the outer ring; arrows shows the direction of the main lobe	Excite probe no. with respect to Fig. 16
Case A		(A, 4) and (B, 1).
Case B		(A, 1) and (B, 1).
Case C		(A, 2) and (B, 1)

3. RESULTS AND DISCUSSION

It is necessary to think of the beam steering antennas as devices with adjustable parameters. For the heterogeneous DRA, positioning the outer ring is the parameter that should be adjusted to change the isolation level between two adjacent antennas for fixed separation; however, for the Multi-feed beam steering DRAs, switching on/off between probes is the parameter that should be controlled to manipulate the radiation pattern and interms changing the isolation level between two adjacent antennas. Even though no direct comparison can be made between the two different beam steering antenna prototypes (heterogeneous and multi-feed), however, the aim of this section is to compare the different isolation levels for the different prototypes at various electrical separations.

Results analysed in previous sections show that the deterioration of return loss and levels of MC are most affected where the direction of the main lobe of antenna A overlaps with the direction of the main lobe of antenna B. Fig. 27 is a plot of the isolation levels versus the different antennas and case studies that have been studied previously. It was found from the simulated results that in the worse case scenario (case 3, heterogeneous DRA), the level of MC between identical heterogeneous beam steering antennas is few dB higher than that that of an omni-directional homogeneous C-DRA (~ 3.3 dB for 0.1 free space wavelength & ~ 2.2 dB for the 0.2 free space wavelength). However a significant isolation level between elements was observed in some scenarios even with the heterogeneous antennas placed in close proximity. For example, a high degree of electrical isolation exists for the heterogeneous DRA case No. 2; more than 25 dB of isolation was achieved even though the two antennas were separated by 0.1 free space wavelength apart. There are two reasons why such isolation exists: First the position of the outer ring in case No. 2 demonstrated that the antenna's main lobe is directed in opposite directions, and hence the level of isolation is high. Second the high permittivity sections of the outer ring of each antenna are facing each others, and hence the electromagnetic interaction is minimum since the sections of the ring with high relative permittivity act as a shield which blocks the electromagnetic wave propagation in that direction; thereby contributing to a higher degree of electrical isolation.

Figure 27 shows that in some scenarios the heterogeneous DRA provides better isolation level compared to the multi-feed beam steering DRA. Even though no direct comparison can be made between case 3 and case C, however evaluating the mutual coupling level of both cases, it can be seen that the multi-feed antenna (case C) has

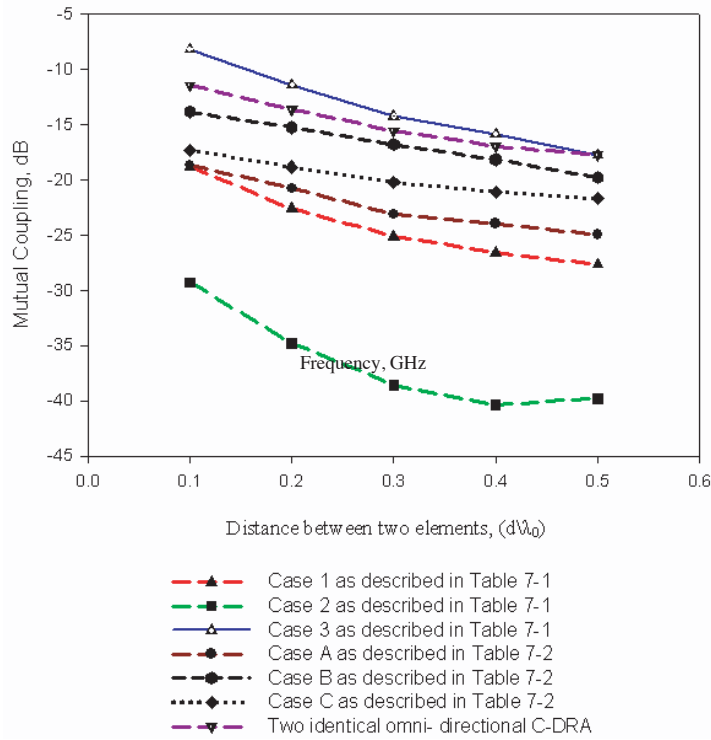


Figure 27. MC versus separation ‘ d ’ for various antenna separations.

better isolation than the heterogeneous DRA (case 3). On the other hand, the far field radiation pattern of the heterogeneous DRA can be controlled over larger range of angles compared to the multi-feed beam steering antenna where its radiation pattern can only be scanned in increments of 90 degrees. Therefore each antenna prototype has its own advantages and drawbacks, and hence a choice between these two prototypes is a trade off between beam scanning capability, isolation level, electrical/mechanical beam steering, speed and separation. The other important parameter that should be considered when evaluating MC of beam steering antennas is the beam-width in the far field pattern; however, this is out of the scope of this current paper.

In addition to changing the location of the outer ring and switching on/off between probes; the other important parameter that affects the coupling mechanism is the displacement between two antennas. The separation between both antennas dictates the level of mutual coupling. Too small a separation between two adjacent elements means a greater electromagnetic interaction between both devices; this was illustrated

in Fig. 27. The expected inverse proportionality between the antennas' separation ' d ' and MC level was also demonstrated.

Even though more scenarios could be considered for the beam steering antennas described previously, however, it is believed that these cases give a good estimation about the isolation levels between the various configurations investigated. Few of the simulated results for the isolation level shown in previous sections (such as the results presented in Fig. 11) were asymmetrical. But running some test simulations with a finer mesh (MC level for case study No. 2 when the electrical separation was 0.1 free space wavelength), it was found that this anomaly was reduced. Also the 'lumpiness' of the S_{21} curves are attributed to mesh artifacts. However, limits on the mesh size were imposed by memory and size and processor time, but the authors believe this did not alter the significant of the report results.

4. CONCLUSION

The antenna arrays described the advantage of using the radiation characteristics of a beam steering DRA to suppress the level of MC between a pair of identical antennas. It has been shown that a significant isolation (< -15 dB) between an array of heterogeneous DRAs can be obtained even with antennas placed in close proximity (0.1 free space wavelength separation). Furthermore it was found that the resonant frequency and return loss are most affected at settings where the direction of the main lobe of antenna A overlaps with the direction of the main lobe of antenna B. The expected inverse proportionality between ' d ' (the separation between two antennas) and the level of MC was also demonstrated.

The information regarding how these antennas should be oriented to suppress the MC between adjacent elements is very interesting and have considerable advantage in designing compact adaptive MIMO system. Lastly at 0.1λ , equivalent to 16 mm at 1.8 GHz, is small enough to fit into a mobile handset.

REFERENCES

1. Chi-Yuk, C., C. Chi-Ho, R. D. Murch, and C. R. Rowell, "Reduction of mutual coupling between closely-packed antenna elements," *IEEE Transactions on Antennas and Propagation*, Vol. 55, 1732–1738, 2007.
2. Browne, D. W., M. Manteghi, M. P. Fitz, and Y. Rahmat-Samii, "Experiments with compact antenna arrays for MIMO

- radio communications,” *IEEE Transactions on Antennas and Propagation*, Vol. 54, 3239–3250, 2006.
3. Fletcher, P. N., M. Dean, and A. R. Nix, “Mutual coupling in multi-element array antennas and its influence on MIMO channel capacity,” *Electronics Letters*, Vol. 39, 342–344, 2003.
 4. Gao, Y., X. Chen, and C. G. Parini, “Channel capacity of dual-element modified PIFA array on small mobile terminal,” *Electronics Letters*, Vol. 43, 1060–1062, 2007.
 5. Rikuta, Y. and H. Arai, “Mutual coupling suppression of two dipole antennas backed by optimized reflector,” *IEE Antennas and Propagation Society International Symposium*, Vol. 2, 276–279, 2002.
 6. Fan, Y. and Y. Rahmat-Samii, “Microstrip antennas integrated with electromagnetic band-gap (EBG) structures: A low mutual coupling design for array applications,” *IEEE Transactions on Antennas and Propagation*, Vol. 51, 2936–2946, 2003.
 7. Kwai-Man, L., L. Wai-Kee, and L. Kwok-Wa, “Mutual impedance of hemispherical dielectric resonator antennas,” *IEEE Transactions on Antennas and Propagation*, Vol. 42, 1652–1654, 1994.
 8. Chair, R., A. A. Kishk, and L. Kai-Fong, “Comparative study on the mutual coupling between different sized cylindrical dielectric resonator antennas and circular microstrip patch antennas,” *IEEE Transactions on Antennas and Propagation*, Vol. 53, 1011–1019, 2005.
 9. Dorris, R. J., R. T. Long, S. A. Long, M. A. A. Khayat, and J. T. A. Williams, “Mutual coupling between cylindrical probed dielectric resonator antennas,” *IEEE Antennas and Wireless Propagation Letters*, Vol. 1, 8–9, 2002.
 10. Fayad, H. and P. Record, “Mechanically steerable fluid dielectric resonator antenna,” *International Journal of Electronics and Communication*, accepted, in press, March 2008.
 11. Fayad, H. and P. Record, “Experimental investigation on new steerable dielectric resonator antenna,” *Electronics Letters*, Vol. 43, 1009–1010, 2007.
 12. Fayad, H. and P. Record, *Adaptive Dielectric Resonator Antenna, Antennas and Propagation Conference, Loughborough, LAPC*, 329–332, 2007.
 13. Fayad, H. and P. Record, “Multi-feed dielectric resonator antenna with reconfigurable radiation pattern,” *Progress In Electromagnetics Research*, PIER 76, 341–356, 2007.